論 文

Improvement of Glass Forming Ability of Ni-Zr-Ti Alloys by Addition of Si and Sn

Jin-Kyu Lee†, Won-Tae Kim* and Do-Hyang Kim**

Abstract

본 연구에서는 Ni-Zr-Ti의 3원계 합금을 기본으로 하여, Si 및 Sn 등의 원소를 첨가하여 Ni-rich 영역에서 벌크 비정질 합금을 제조하였다. $Ni_{59}Zr_{20}Ti_{16}Si_2Sn_3$ 조성의 합금에서 injection casting에 의하여 약 58 K의 과냉각액상영역을 가지고 있는 직경 3 mm의 벌크 비정질 시편을 제조하였다. 이러한 우수한 비정질 형성능은 액상온도의 저하로 인해 낮은 온도까지 액상이 쉽게 과냉되기 때문인 것으로 사료된다. $Ni_{59}Zr_{20}Ti_{16}Si_5$ 합금은 두 단계에 걸쳐 결정화가 일어나는 반면, $Ni_{59}Zr_{20}Ti_{16}Si_2Sn_3$ 합금은 단일 단계에 의해 orthorhombic $Ni_{10}(Zr,Ti)_7$ 결정상과 cubic NiTi 결정상으로 결정화가 일어난다. 벌크 비정질 $Ni_{59}Zr_{20}Ti_{16}Si_2Sn_3$ 합금의 경우 압축강도는 2.7 GPa, 연신율은 약 2% 정도의 값을 가진다.

Keywords: Ni-based, Bulk amorphous, Glass forming ability, Mechanical property (Received April 12, 2003)

1. Introduction

Bulk amorphous alloys exhibit many unique properties associated with the atomic structure.[1] These unique properties that can be rarely found in crystalline materials are attractive for the practical applications as new classes of structural as well as functional materials. Several bulk amorphous alloys have been developed mainly in the Zr-based,[2] Ti-based,[3] and Mg-based alloy systems.[4] This renewed interests in bulk glass formation for both scientific and engineering reasons. Some Zr-based bulk amorphous alloys can be produced by a conventional casting process leading to successful applications of the amorphous alloys for sporting goods. However, due to the limit of Zr resources, development of bulk amorphous alloys containing common metals as major consistent is strongly desired for the extensive practical applications of bulk amorphous alloys.

Development of Ni-based bulk amorphous alloys is expected to expand the application fields of the amorphous alloys. Many Ni-based amorphous alloys have been produced through rapid quenching techniques.[5,6] Nevertheless, Ni-based bulk amorphous alloys have been reported in a few alloy systems, for example, the Ni-Nb-Cr-Mo-P-B alloy[7] and Ni-Zr-Ti-Si alloy.[8,9] Fully amorphous rods with the maximum diameter of 1 mm have been prepared in the Ni-Nb-Cr-Mo-P-B system.[7] Since the glass forming ability (GFA) of the Ni-based amorphous alloys can be effectively improved by the addition of P or B, large amount additions of P and B (~20 at% in total) are necessary for the enhanced GFA of the Ni-Nb-Cr-Mo-P-B alloys.[7] However, the temperature range for practical appli-cations can be limited to lower temperature since the glass transition temperature, T_g tends to decrease as the amount of the metalloid elements increases. Recently, Ni-Zr-Ti-Si alloys without addition of B and P are reported to have a high glass forming ability. Fully amorphous rods with the diameter of 2 mm have been prepared in Ni-Zr-Ti-Si alloys.[8,9]

The main aim of this work is to the develop a new class of Ni-based amorphous alloys in the Ni-Ti-Zr

한국생산기술연구원 신소재본부 나노소재팀(Nano Material Team, Advanced Material R&D center, Korea Institute of Industrial Technology)
*청주대학교 응용과학부(Division of Applied Science, Chongju University)
**연세대학교 신소재공학부 준결정재료연구단(Center for Noncrystalline Materials, School of Advanced Material Engineering, Yonsei University)
†E-mail : jklee@kitech.re.kr

system by small addition of Si, Sn or simultaneous addition of Si and Sn. Sn has large negative heat of mixing with the metallic elements. Si can also be considered since it has intermediate atomic radius (Ni < Si < Ti < Zr) and large heats of mixing with the metallic elements Ni, Ti and Zr.[8] Moreover, Si and Sn are much cheaper and easier to be inductively melted than P. In the present study the bulk amorphous alloys are prepared by injection casting method. The mechanical properties of the bulk amorphous alloys are investigated.

2. Experimental

Alloys of nominal composition $Ni_{59}Zr_{20}Ti_{21}$, $Ni_{59}Zr_{20}Ti_{16}Si_5$ and $Ni_{59}Zr_{20}Ti_{16}Si_2Sn_3$ were prepared by arc melting of high pure metals; Ni(99.99%), Zr(99.9%), Ti(99.97%), Si(99.999%) and Sn(99.999%) under an argon atmosphere. Amorphous alloy specimens were produced by melt-spinning and injection casting methods under an Ar atmosphere. For melt-spinning, the alloys were remelted in quartz tubes, followed by ejecting with an over pressure of 35 kPa through a nozzle onto a Cu wheel rotating with a surface velocity of 40 m/s. The resulting ribbons exhibit thickness of about 30 μm and width of about 2 mm. Bulk amorphous rod specimens of 3 mm in diameter were fabricated by injection casting. The $Ni_{59}Zr_{20}Ti_{16}Si_2Sn_3$ alloy was remelted in quartz tubes, followed by casting into a 3 mm diameter cylindrical cavity of a Cu mold. Heat treatment of the amorphous specimens was preformed under an Ar atmosphere at several different conditions depending on alloys. Structural change during the heat treatment was studied by using X-ray diffractometry with monochromatic Cu Kα radiation (Rigaku, RINT2200). Thermal analysis of the amorphous samples was carried out by a differential scanning calorimetry (Perkin Elmer, DSC 7). DSC traces were monitored during continuous heating from 298 to 983 K at a constant heating rate of 0.33 K/s. Also differential thermal analysis (Prrkin Elmer, DTA 7) was performed to measure the temperature range of alloy melting endotherms during continuous heating with a constant heating rate of 0.33 K/s. From the cast rods, cylindrical specimens with sizes of Φ1 × 2.5 mm were prepared and uniaxial compression test were conducted under the constant cross-head speed condition (Initial strain rate = 1×10^{-4} s^{-1}) on an Instron-type machine.

3. Results

Figure 1 shows DSC traces obtained during continuous heating at a heating rate of 0.33 K/s for the ribbon $Ni_{59}Zr_{20}Ti_{21}$, $Ni_{59}Zr_{20}Ti_{16}Si_5$ and $Ni_{59}Zr_{20}Ti_{16}Si_2Sn_3$ alloys. The DSC trace from the melt-spun $Ni_{59}Zr_{20}Ti_{21}$ alloy exhibited an endothermic event corresponding to glass transition to supercooled liquid, and two overlapped exothermic peaks corresponding to crystallization of the supercooled liquid. The alloy showed glass transition temperature (T_g) of 794 K, onset temperature of the first exotherm (T_{X1}) of 808 K and integrated heat of crystallization of 65.3 J/g. The supercooled liquid range, defined as $\Delta T_X = T_{X1} - T_g$, is about 14 K. The $Ni_{59}Zr_{20}Ti_{16}Si_5$ and $Ni_{59}Zr_{20}Ti_{16}Si_2Sn_3$ alloys exhibit significantly different thermal behavior from the ternary $Ni_{59}Zr_{20}Ti_{21}$ alloy. The DSC trace for the melt spun $Ni_{59}Zr_{20}Ti_{16}Si_5$ alloy exhibits a glass transition at 830 K, followed by two exothermic peaks with onset temperatures and exothermic heats of 876 K and 35.1 J/g for the first strong exotherm and 927 K and 10.6 J/g for the second weak exotherm,

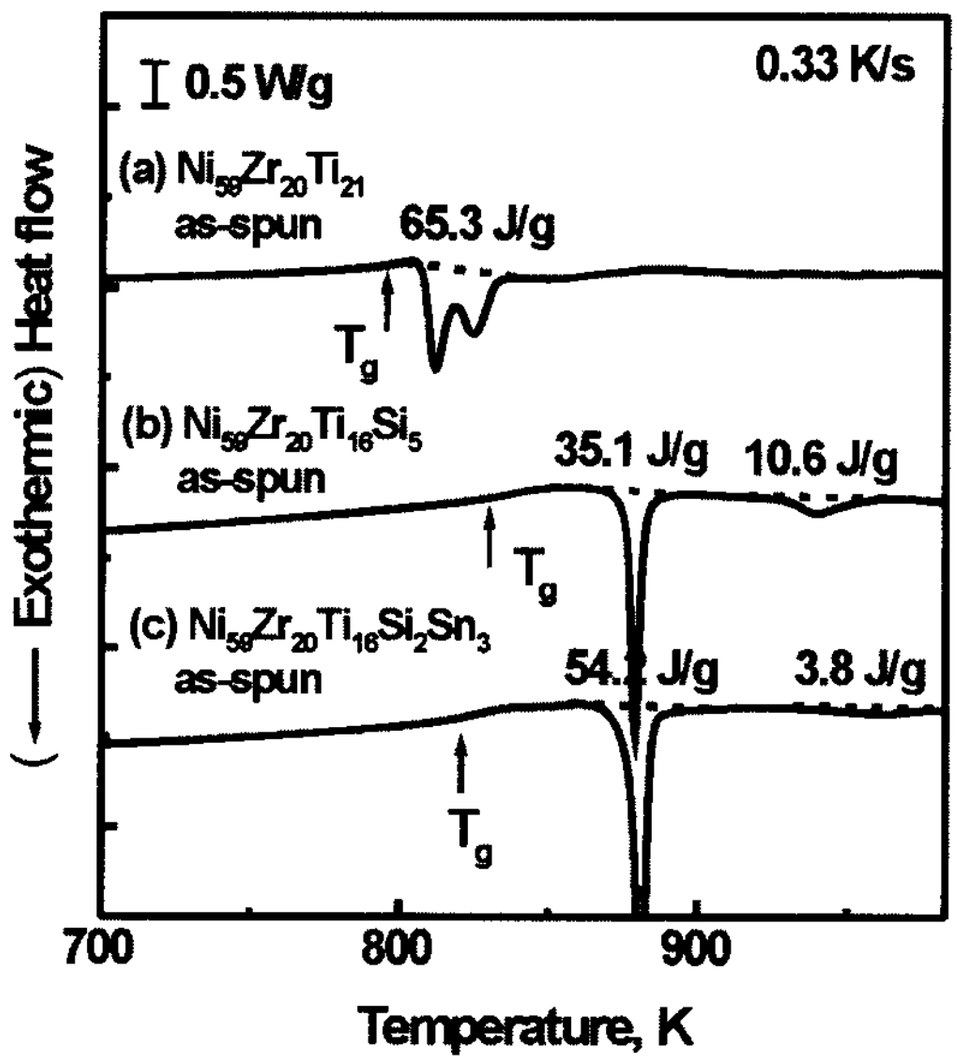

Fig. 1. Typical DSC traces obtained during continuous heating rate of 0.33 K/s: (a) as-spun $Ni_{59}Zr_{20}Ti_{21}$; (b) as-spun $Ni_{59}Zr_{20}Ti_{16}Si_5$; and (c) as-spun $Ni_{59}Zr_{20}Ti_{16}Si_2Sn_3$.

respectively. The amorphous $Ni_{59}Zr_{20}Ti_{16}Si_2Sn_3$ alloy exhibits a glass transition at 820 K and two exothermic peaks. The onset temperatures and exothermic heats of two exothermic peaks are 878 K and 54.2 J/g for the first strong exotherm and 939 K and 3.8 J/g for the second weak exotherm, respectively. ΔT_x of the $Ni_{59}Zr_{20}Ti_{16}Si_5$ and $Ni_{59}Zr_{20}Ti_{16}Si_2Sn_3$ alloy are about 46 and 58 K, respectively, which is significantly larger than that of the ternary $Ni_{59}Zr_{20}Ti_{21}$ alloy.

Figure 2 shows typical DSC spectra obtained during continuous heating at a heating rate of 0.33 K/s for the melt-spun and injection-cast $Ni_{59}Zr_{20}Ti_{16}Si_5$ and $Ni_{59}Zr_{20}Ti_{16}Si_2Sn_3$ alloys. Injection-cast $Ni_{59}Zr_{20}Ti_{16}Si_5$ and $Ni_{59}Zr_{20}Ti_{16}Si_2Sn_3$ alloys show almost same crystallization behavior as the ribbon specimen. The integrated heat of the exotherms for the bulk specimen is almost same as that in the melt-spun specimen, indicating fully amorphous structure was obtained in the injection-cast specimen. The formation of the amorphous phase was confirmed by XRD and TEM.

Figure 3 shows DTA traces obtained from the melt-spun $Ni_{59}Zr_{20}Ti_{21}$, $Ni_{59}Zr_{20}Ti_{16}Si_5$ and $Ni_{59}Zr_{20}Ti_{16}Si_2Sn_3$ alloys during continuous heating at a heating rate of 0.33 K/s. The solidus temperature (T_m^{sol}) and liquidus

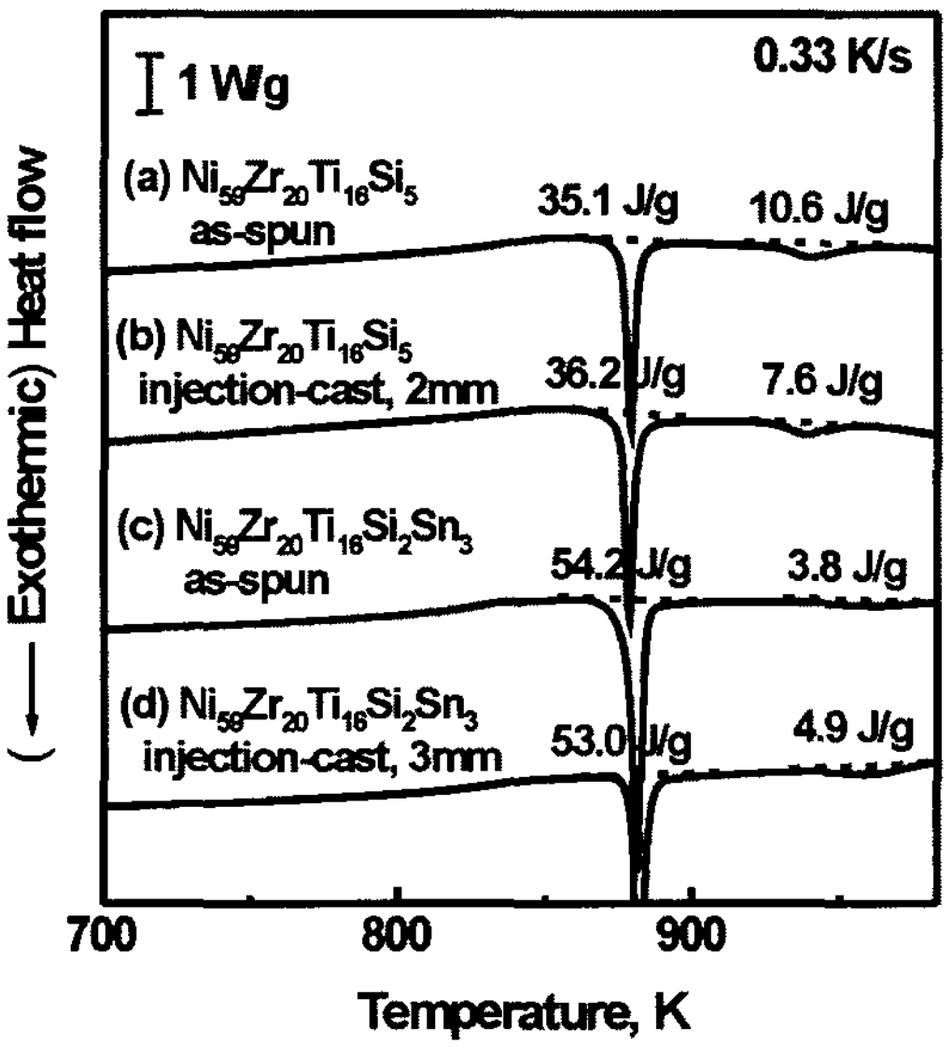

Fig. 2. Typical DSC spectra obtained during continuous heating rate of 0.33 K/s: (a) as-spun $Ni_{59}Zr_{20}Ti_{16}Si_5$; (b) injection -cast $Ni_{59}Zr_{20}Ti_{16}Si_5$; (c) as-spun $Ni_{59}Zr_{20}Ti_{16}Si_5$; and (d) injection-cast $Ni_{59}Zr_{20}Ti_{16}Si_2Sn_3$.

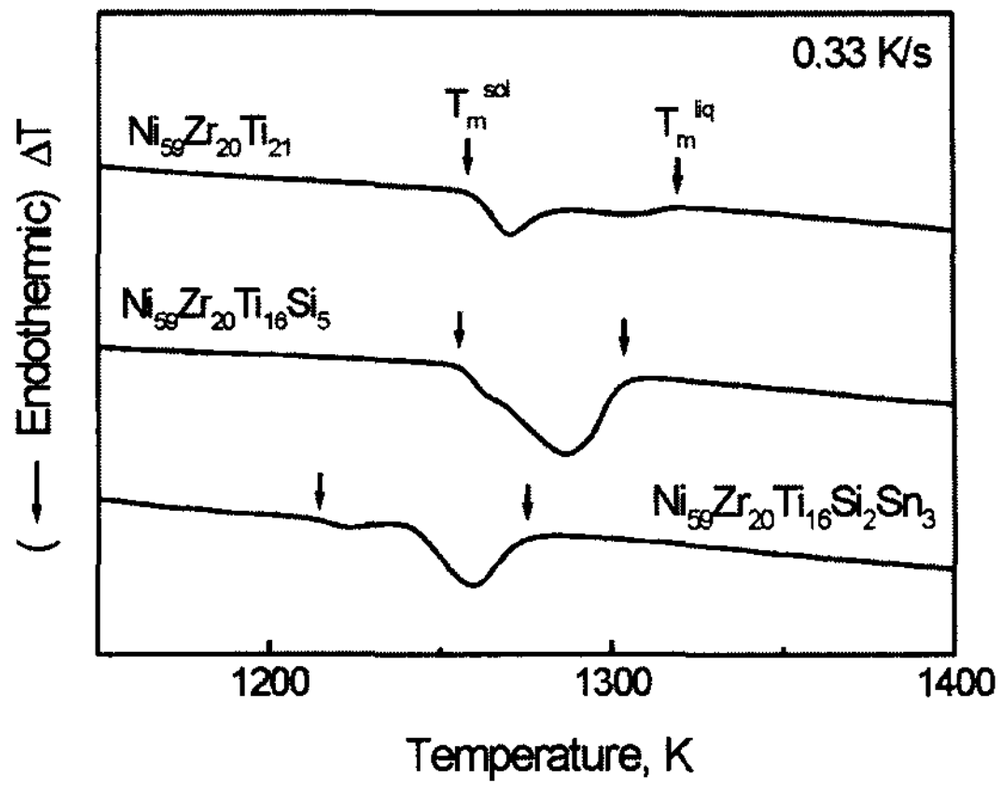

Fig. 3. Typical DTA traces obtained from melt-spun $Ni_{59}Zr_{20}Ti_{21}$, $Ni_{59}Zr_{20}Ti_{16}Si_5$ and $Ni_{59}Zr_{20}Ti_{16}Si_2Sn_3$ samples during continuous heating.

temperature (T_m^{liq}) assumed to be the onset and end temperature, respectively, of the melting endotherm. The $Ni_{59}Zr_{20}Ti_{16}Si_2Sn_3$ alloy exhibits the lowest T_m^{sol} (= 1213 K) and T_m^{liq} (= 1272 K) among the investigated alloys.

In order to identify the crystallization products for each exothermic reaction, annealing treatments were performed under two conditions: i) to complete the first exothermic reaction; and ii) to complete the final exothermic reaction. Figure 4 shows typical XRD traces obtained from the melt-spun and annealed the $Ni_{59}Zr_{20}Ti_{16}Si_5$ and the $Ni_{59}Zr_{20}Ti_{16}Si_2Sn_3$ ribbon specimens. Crystallization sequence of the $Ni_{59}Zr_{20}Ti_{16}Si_5$ amorphous alloy was completely different from that of the $Ni_{59}Zr_{20}Ti_{16}Si_2Sn_3$ amorphous alloy. The XRD trace of the $Ni_{59}Zr_{20}Ti_{16}Si_5$ specimen annealed for 10 s at 903 K, shows sharp diffraction peaks superimposed on a weak halo pattern, indicating partial crystallization occurs. The first crystallization exotherm of the $Ni_{59}Zr_{20}Ti_{16}Si_5$ alloy corresponds to primary crystallization of amorphous phase into a cubic NiTi phase with a lattice constant of a = 0.301 nm in the amorphous matrix. The XRD trace from the specimen annealed for 60 s at 983 K, shows several sharp diffraction peaks. All the diffraction peaks could be analyzed into a mixture of orthorhombic $Ni_{10}(Zr,Ti)_7$ with lattice constants a = 0.921 nm, b = 0.916 nm, c = 1.239 nm and cubic NiTi phases. In the case of the $Ni_{59}Zr_{20}Ti_{16}Si_2Sn_3$ alloy orthorhombic $Ni_{10}(Zr,Ti)_7$ and the cubic NiTi phases are simultaneously crystallized from the amorphous matrix

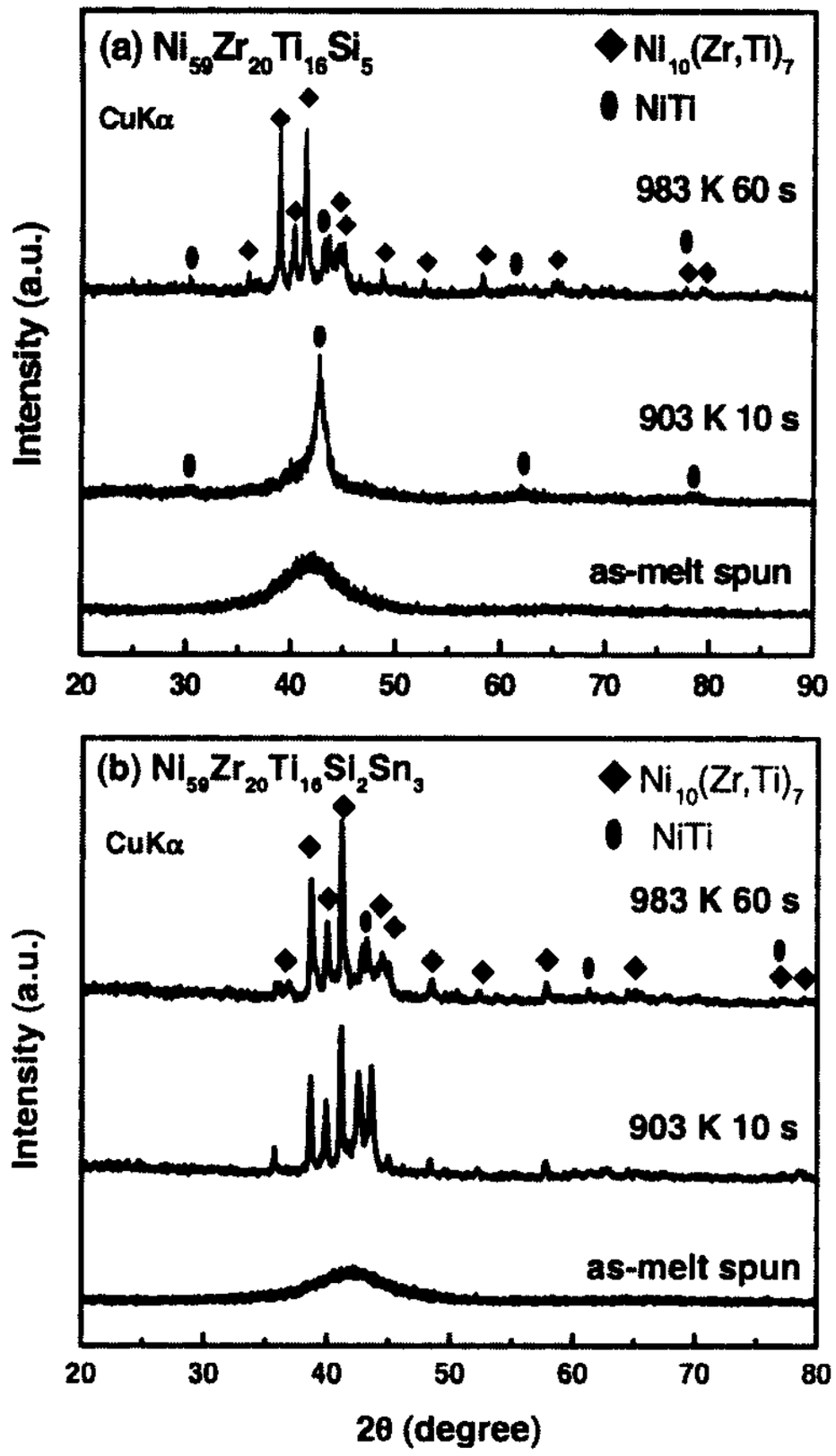

Fig. 4. Typical XRD traces obtained from as-spun and annealed (a) $Ni_{59}Zr_{20}Ti_{16}Si_5$; and (b) $Ni_{59}Zr_{20}Ti_{16}Si_2Sn_3$ specimen.

and grow without forming any other crystalline phases upon further annealing treatment, as can be seen in Figure 3(b). In the present study, the phase formed after the second exotherm in the DSC spectra (Figure 1(c)) could not be clearly identified.

Figure 5 shows the uniaxial compressive stress-strain curves of the cast $Ni_{59}Zr_{20}Ti_{16}Si_5$ and $Ni_{59}Zr_{20}Ti_{16}Si_2Sn_3$ alloy rods deformed under the constant cross-head speed condition (initial strain rate = 1×10^{-4} s^{-1}). Both alloys show linear elastic behavior up to yielding and then maintain the almost constant stress level during plastic deformation. The compressive fracture strength and plastic strain are approximately 2700 MPa and 2.1%, respectively, for the amorphous $Ni_{59}Zr_{20}Ti_{16}Si_5$ alloy, and 2659 MPa and 1.9%, respectively, for the $Ni_{59}Zr_{20}Ti_{16}Si_2Sn_3$ alloy.

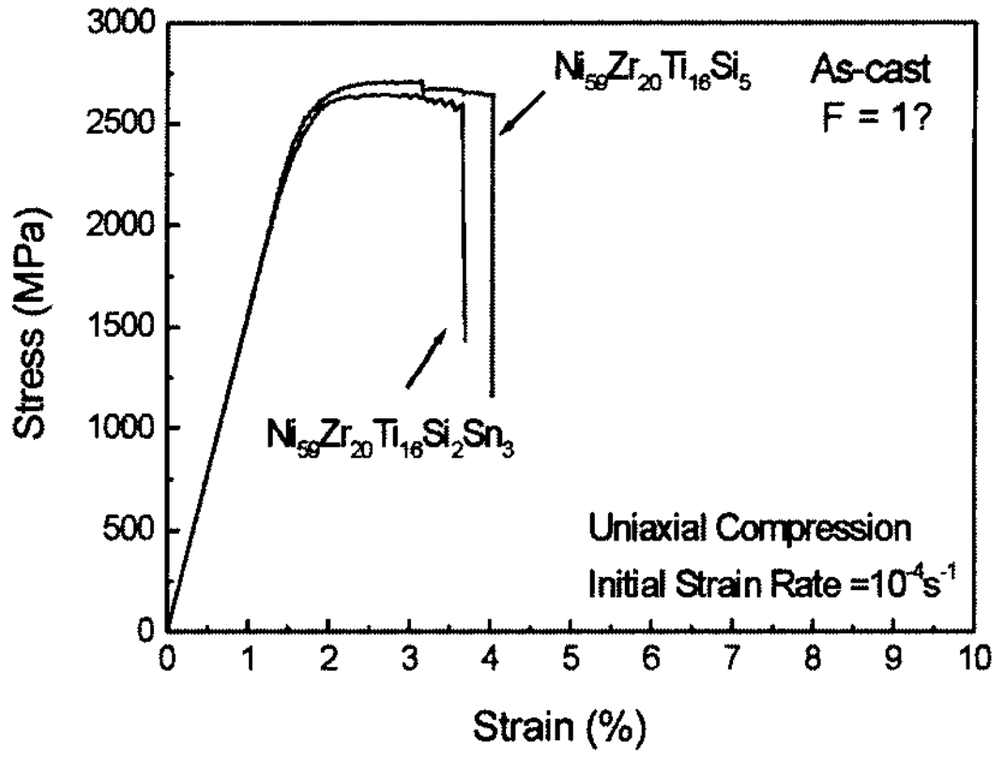

Fig. 5. Compressive stress-strain curves of the amorphous $Ni_{59}Zr_{20}Ti_{16}Si_5$ and $Ni_{59}Zr_{20}Ti_{16}Si_2Sn_3$ alloy rods with a diameter of 1 mm.

4. Discussion

The quaternary alloys exhibit much better thermal stability than that of ternary alloy. The amorphous $Ni_{59}Zr_{20}Ti_{16}Si_5$ alloy exhibits higher T_g, T_{X1} and larger ΔT_x than those of the $Ni_{59}Zr_{20}Ti_{21}$ alloy by 36, 38 and 32 K, respectively. These increments in glass transition and crystallization temperatures by partial replacement of Ti by Si can be understood based on the large interaction energy of Ti-Si and Zr-Si atomic pairs. The atomic size effect on the glass forming ability is not expected to be high. The mixing enthalpies of Ni-Si, Ti-Si and Zr-Si atomic pairs are estimated to be 23, -59 and 67 kJ/mol, respectively.[10]

The strong interaction of Ti-Si and Zr-Si atomic pairs may contribute to stabilize the amorphous phase. Due to the formation of the strong atomic pairs, atomic rearrangement for glass transition and for nucleation and growth of crystalline phase in the supercooled liquid phase is kinetically retarded and thus, the ΔT_x is enlarged.

The $Ni_{59}Zr_{20}Ti_{16}Si_2Sn_3$ alloy exhibits the largest ΔT_x (= 56 K) among the alloys investigated, and the alloy shows the highest GFA up to the diameter of 3 mm. The largest diameter cast with fully amorphous phase has been considered as a real parameter reflecting the GFA of the alloy since the critical cooling rate (R_c) in inversely proportional to this dimension.[11] For the $Ni_{59}Zr_{20}Ti_{16}Si_2Sn_3$ alloy, the increase of GFA may be explained based on

the following: (1) higher order multi-component system, (2) large difference in atomic size between Sn and other constituent elements, (3) large interaction energy between Si and other constituent elements.

To get an amorphous phase during solidification, the nucleation and growth of a competing crystalline phase should be prevented in the temperature range between T_m^{liq} and T_g at lower cooling rate. The glass forming ability is usually determined by the stability of the alloy at this temperature range. The more stable an alloys is at this temperature range, the lower critical cooling rate for glass formation and the better the glass forming ability. This temperature range can be presented by using $T_{rg} = T_g/T_m^{liq}$, which has been generally found to be a good indicator of GFA.[12] As shown earlier in Fig. 3, the difference between T_m^{liq} and T_g is a minimum in the amorphous $Ni_{59}Zr_{20}Ti_{16}Si_2Sn_3$ alloy, which lead to higher GFA up to the diameter of 3 mm. Therefore, lower cooling rate due to a decrease of liquidus temperature leads to better GFA in the amorphous $Ni_{59}Zr_{20}Ti_{16}Si_2Sn_3$ alloy.

5. Conclusion

New Ni-based bulk amorphous alloys are developed through systematic alloy design based upon the empirical rules for high glass forming alloys. Small replacements of Ti by Si or Sn greatly improve the glass forming ability of $Ni_{59}Ti_{21}Zr_{20}$ alloys. The bulk amorphous $Ni_{59}Zr_{20}Ti_{16}Si_2Sn_3$ alloy with diameter of 3 mm is fabricated by injection casting. The amorphous $Ni_{59}Zr_{20}Ti_{16}Si_5$ alloy crystallized through two-step reactions. First, primary crystallization of a cubic NiTi phase occurred from the amorphous matrix and then the NiTi and remaining amorphous phase transformed into a mixture of cubic NiTi and orthorhombic $Ni_{10}(Zr,Ti)_7$ phase. On the other hand, the amorphous $Ni_{59}Zr_{20}Ti_{16}Si_2Sn_3$ alloy crystallized via simultaneous precipitation of orthorhombic $Ni_{10}(Zr,Ti)_7$ and NiTi phases. These Ni-based bulk amorphous alloys exhibit good mechanical properties, high compressive fracture strength of about 2700 MPa with a macroscopic plastic strain of about 2.0%.

Acknowledgement

This work was supported by the Creative Research Initiatives of the Korean Ministry of Science and Technology.

References

[1] A. Inoue : Acta Mater., "Stabilization of metallic supercooled liquid and bulk amorphous alloys", 48 (2000) 279-306.

[2] A. Peker and W. L. Johnson : Appl. Phys. Lett., "A highly processable metallic glasses": $Zr_{41.2}Ti_{13.8}Cu_{12.5}Ni_{10.0}Be_{22.5}$ 63 (1993) 2342-2344.

[3] T. Zhang and A. Inoue : Mater. Trans. JIM, "Preparation of Ti-Cu-Ni-Si-B amorphous alloys with a large supercooled liquid region", 40 (1999) 301-306.

[4] E. S. Park, H. G. Kang, W. T. Kim and D. H. Kim : J. Non-Cryst. Solids, "The effect of Ag addition on the glass forming ability of Mg-Cu-Y metallic glass alloys", 279 (2001) 154-160.

[5] S. Budurov, V. Fotty, S. Toncheva, and R. Kovacheva : Mater. Sci. Eng. A, "The glass forming ability in the ternary Ni-Co-P and Ni-Cu-P systems", 133 (1991) 455-457.

[6] T. G. Park, S. Yi, and D. H. Kim : Scripta Mater., "Development of new Ni-based amorphous alloys containing no metalloid that have large undercooled liquid regions", 43 (2000) 109-114.

[7] X. Wang, I. Yoshii, A. Inoue, Y. H. Kim and I. B. Kim : Mater. Trans. JIM, "Bulk amorphous $Ni_{75-x}Nb_5M_xP_{20-y}B_y$ (M=Cr,Mo) alloys with large supercooling and high strength", 40 (1999) 1130-1136.

[8] S. Yi, J. K. Lee, W. T. Kim and D. H. Kim : J. Non-Cryst. Solids, "Ni-based bulk amorphous alloys in the Ni-Ti-Zr-Si system", 291 (2001) 132-136.

[9] J. K. Lee, S. H. Kim, S. Yi, W. T. Kim and D. H. Kim : Mater. Trans. JIM, "A study on the development of Ni-based alloys with wide supercooled liquid region", 42 (2001) 592-596.

[10] F. R. Boer, R. Boom, W. C. M. Mattens, A. R. Miedema and A. K. Niessen : "Cohesion in metals", North-Holland, Amsterdam, (1989) 291-336.

[11] X. H. Lin and W. L. Johnson : J. Appl. Phys., "Formation of Ti-Zr-Cu-Ni bulk metallic glasses", 10 (1995) 6514-6519.

[12] D. Turnbull : "Solid state physics, Academic", New York, (1956) 225.